

## Modular Strategy for the Construction of Radiometalated Antibodies for Positron Emission Tomography Based on Inverse Electron Demand Diels–Alder Click Chemistry

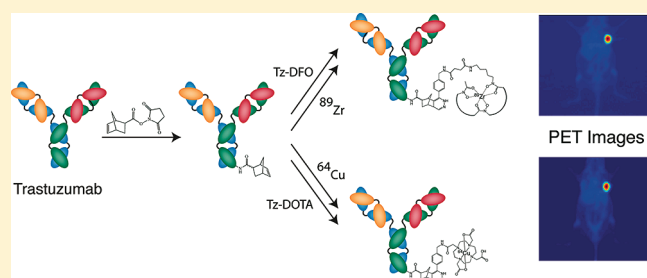
Brian M. Zeglis,<sup>†</sup> Priya Mohindra,<sup>†</sup> Gabriel I. Weissmann,<sup>†</sup> Vadim Divilov,<sup>†</sup> Scott A. Hilderbrand,<sup>†</sup> Ralph Weissleder,<sup>‡</sup> and Jason S. Lewis<sup>\*†</sup>

<sup>†</sup>Department of Radiology and the Program in Molecular Pharmacology and Chemistry, Memorial Sloan-Kettering Cancer Center, New York, New York, United States

<sup>‡</sup>Center for Systems Biology, Massachusetts General Hospital/Harvard Medical School, Boston, Massachusetts, United States

**S** Supporting Information

**ABSTRACT:** A modular system for the construction of radiometalated antibodies was developed based on the bioorthogonal cycloaddition reaction between 3-(4-benzylamino)-1,2,4,5-tetrazine and the strained dienophile norbornene. The well-characterized, HER2-specific antibody trastuzumab and the positron emitting radioisotopes <sup>64</sup>Cu and <sup>89</sup>Zr were employed as a model system. The antibody was first covalently coupled to norbornene, and this stock of norbornene-modified antibody was then reacted with tetrazines bearing the chelators 1,4,7,10-tetraazacyclo-dodecane-1,4,7,10-tetraacetic acid (DOTA) or desferrioxamine (DFO) and subsequently radiometalated with <sup>64</sup>Cu and <sup>89</sup>Zr, respectively. The modification strategy is simple and robust, and the resultant radiometalated constructs were obtained in high specific activity (2.7–5.3 mCi/mg). For a given initial stoichiometric ratio of norbornene to antibody, the <sup>64</sup>Cu-DOTA- and <sup>89</sup>Zr-DFO-based probes were shown to be nearly identical in terms of stability, the number of chelates per antibody, and immunoreactivity (>93% in all cases). *In vivo* PET imaging and acute biodistribution experiments revealed significant, specific uptake of the <sup>64</sup>Cu- and <sup>89</sup>Zr-trastuzumab bioconjugates in HER2-positive BT-474 xenografts, with little background uptake in HER2-negative MDA-MB-468 xenografts or other tissues. This modular system—



one in which the divergent point is a single covalently modified antibody stock that can be reacted selectively with various chelators—will allow for both greater versatility and more facile cross-comparisons in the development of antibody-based radiopharmaceuticals.

### INTRODUCTION

Over the past two decades, radiopharmaceuticals based on antibodies have assumed an increasingly prominent role in both diagnostic and therapeutic nuclear medicine. This trend is particularly evident in the field of positron emission tomography (PET), in which a wide variety of effective antibody-based radiotracers have been developed against an array of cancer biomarkers.<sup>1–3</sup> Indeed, while some promising imaging agents have been labeled with long-lived nonmetallic radionuclides such as <sup>124</sup>I, the majority of antibody-based PET bioconjugates have employed positron-emitting radiometals, including <sup>64</sup>Cu, <sup>86</sup>Y, and, most recently, <sup>89</sup>Zr.<sup>4–8</sup> In these systems, radiometals offer significant advantages over their nonmetallic cousins, most notably decay characteristics that result in high image quality, radioactive half-lives that complement the biological half-lives of the antibody vectors, and enhanced control and ease of radiolabeling through the use of chelating moieties.

Despite their benefits, however, these chelating moieties are the source of a somewhat confounding issue in the study of radiometalated antibodies. Put simply, different radiometals

require different chelators. For example, the small, hard <sup>89</sup>Zr<sup>4+</sup> cation shows very high affinity for the multiple oxygen donors of the chelator desferrioxamine (DFO), while the larger and softer <sup>64</sup>Cu<sup>2+</sup> cation exhibits higher thermodynamic and kinetic stability when bound to chelators bearing nitrogen donors in addition to oxygens, for example, 1,4,7,10-tetraazacyclo-dodecane-1,4,7,10-tetraacetic acid (DOTA) and 1,4,8,11-tetraazabicyclo[6.6.2]hexadecane-4,11-diyl)diacetic acid (CB-TE2A).<sup>6,9</sup> Further, different chelators often require dramatically different synthetic strategies for antibody couplings.<sup>10</sup> In an isolated case of one antibody and one radiometal, these facts do not present a problem. However, they do create a significant obstacle to the versatility of radiometalated bioconjugates. To wit, given a particular monoclonal antibody, the development of a <sup>64</sup>Cu-CB-TE2A-mAb conjugate for PET, a <sup>89</sup>Zr-DFO-mAb conjugate for PET, and a <sup>225</sup>Ac-DOTA-mAb conjugate for therapy would require three different routes

**Received:** June 4, 2011

**Revised:** August 22, 2011

**Published:** August 31, 2011

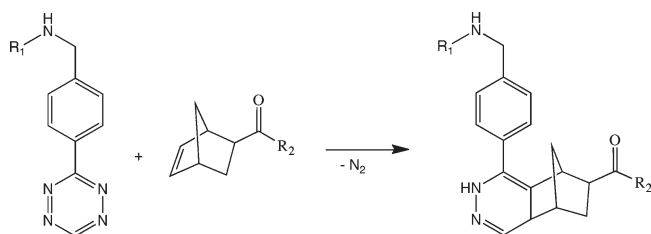


**Figure 1.** Tetrazine–norbornene ligation.

for antibody modification. Not only would this require additional time to develop and optimize each pathway, but the disparate routes would also mandate differing reaction conditions for each antibody, opening the door for differences in immunoreactivity and chelator/antibody ratio and ultimately making meaningful comparisons among the various radiopharmaceuticals more difficult. Consequently, a modular system—one in which the divergent point is a single covalently modified antibody stock that can be reacted selectively with various chelators—would resolve these issues and allow for more versatility and cross-comparisons in the development of antibody-based radiopharmaceuticals.

The chemical requirements of such a modular system—selectivity, biocompatibility, bioorthogonality—make it an almost perfect application for the use of click chemistry. Coined by K. Barry Sharpless, the term “click chemistry” broadly defines a group of chemical reactions by which two molecular components can be joined via a selective, rapid, clean, bioorthogonal, and biocompatible ligation.<sup>11–13</sup> By far, the most popular example of click chemistry is the Cu(I)-catalyzed [3 + 2] Huisgen cycloaddition between an azide and alkyne.<sup>14</sup> This reaction has already been widely employed in the development of radiotracers, particularly <sup>18</sup>F-based PET probes.<sup>15–18</sup> The application of this technology to radiometal-based probes has lagged behind, however, most likely due to concerns over metal contamination by the catalyst itself, though “clickable” chelators based on both the Cu(I)-catalyzed reaction and other Cu(I)-free systems have become more common in the literature in recent years.<sup>19–22</sup> Very recently, another promising “click” variant has come to light: the inverse electron demand Diels–Alder reaction between a tetrazine moiety and a strained alkene dienophile (Figure 1).<sup>23–25</sup> Like other click reactions, the ligation is selective, fast, biocompatible, and bioorthogonal, and unlike many Diels–Alder reactions, the coupling is irreversible, forming stable pyridazine products after the retro-Diels–Alder release of dinitrogen from the reaction intermediate. A number of different tetrazine-strained alkene pairs have been explored for the reaction, though the combination of 3-(4-benzylamino)-1,2,4,5-tetrazine (Tz) and either norbornene- or trans-cyclooctene-derivatives seems well-suited for biological applications. To date, the ligation has been employed in a variety of settings: the modification of oligonucleotides;<sup>26</sup> fluorescence imaging with small molecules, antibodies, and nanoparticles;<sup>23,24,27,28</sup> SPECT imaging with antibodies;<sup>29</sup> and <sup>18</sup>F-PET imaging with peptides.<sup>30,31</sup> However, to the best of the authors’ knowledge, no application of this technology to positron-emitting radiometals has yet been made.

Herein, we report the development of a modular strategy for the construction of radiolabeled antibodies using the tetrazine–norbornene click reaction. The synthetic pathway involves three simple steps: (1) creation of a common stock of norbornene-modified antibody via peptide coupling; (2) ligation of a chelator-modified

tetrazine moiety to the norbornene-modified antibody; and (3) radiolabeling of the resultant construct (Figure 2). For this proof of concept investigation, we have chosen the positron-emitting radiometals <sup>64</sup>Cu and <sup>89</sup>Zr, the chelators DOTA and DFO, and the antibody trastuzumab. <sup>64</sup>Cu and <sup>89</sup>Zr are the two most common radionuclides employed in antibody-based PET bioconjugates, and DOTA and DFO, respectively, are the most common chelators employed with these two metals.<sup>6,9,10,32–34</sup>

The antibody at hand, trastuzumab (Herceptin, Genentech), is an extremely well-characterized antibody specific to the human epidermal growth factor receptor 2 (HER2, also known as ERBB2). Overexpression of HER2 has been shown to be associated with augmented metastatic potential, increased tumor aggression, and poor prognosis for disease-free survival for patients with a variety of malignancies, most notably breast, ovarian, and colorectal cancer.<sup>35–38</sup> Trastuzumab alone has been employed as a therapeutic agent, and conjugates of both the antibody and its derivative fragments have been synthesized bearing a wide variety of radionuclides—including <sup>64</sup>Cu, <sup>86</sup>Y, <sup>111</sup>In, <sup>124</sup>I, <sup>99m</sup>Tc, and <sup>89</sup>Zr—for PET and SPECT imaging of HER2 expression.<sup>39–47</sup> It is our hope that this modular methodology will aid in both the expansion of the comparative study of antibodies labeled with different radionuclides and the development of novel antibody-based radiopharmaceuticals. Since more and more antibodies and dienophiles are being developed, this modular approach will likely lead to the rapid development of many novel imaging agents.<sup>28</sup> Importantly, while we have used positron-emitting radionuclides in this study due to our laboratory’s area of expertise, this modular system need not be applied only to PET radiometals but rather can be used across the spectrum of metallic radionuclides, encompassing those employed for SPECT and radiotherapy as well.

## EXPERIMENTAL PROCEDURES

**Materials.** All chemicals, unless otherwise noted, were acquired from Sigma-Aldrich (St. Louis, MO) and were used as received without further purification. All water employed was ultrapure (>18.2 MΩ cm<sup>-1</sup> at 25 °C, Milli-Q, Millipore, Billerica, MA), and was passed through a 10 cm column of Chelex resin (Bio-Rad Laboratories, Hercules, CA) before use. DMSO was of molecular biology grade (>99.9%: Sigma, D8418), and all other solvents were of the highest grade commercially available. 1,4,7,10-Tetraazacyclododecane-1,4,7,10-tetraacetic acid mono-*N*-hydroxysuccinimidylester (DOTA-NHS) was purchased from Macrocylics Inc. (Dallas, TX). *N*-Succinyl-desferrioxamine B was prepared according to published procedures.<sup>48</sup> All instruments were calibrated and maintained in accordance with standard quality-control procedures.<sup>49</sup> UV–vis measurements were taken on a Cary 100 Bio UV–vis spectrophotometer. NMR spectroscopy was performed on a Bruker 500 MHz NMR with *Topsin 2.1* software for spectrum analysis. HPLC was performed using a Shimadzu HPLC equipped with a C-18 reversed-phase column (Phenomenex Luna analytical 4.6 × 250 mm or Semi-Prep 21.2 × 100 mm, 5 μm, 1.0 or 6.0 mL/min), 2 LC-10AT pumps, a SPD-M10AVP photodiode array detector, and a gradient of 0:100 MeCN/H<sub>2</sub>O (both with 0.1% TFA) to 100:0 MeCN/H<sub>2</sub>O over 15 min].

<sup>64</sup>Cu was purchased from Washington University, St. Louis, where it was produced on the Washington University School of Medicine Cyclotron (model CS-15, Cyclotron Corp.) by the <sup>64</sup>Ni(*p,n*)<sup>64</sup>Cu reaction and purified as previously described to

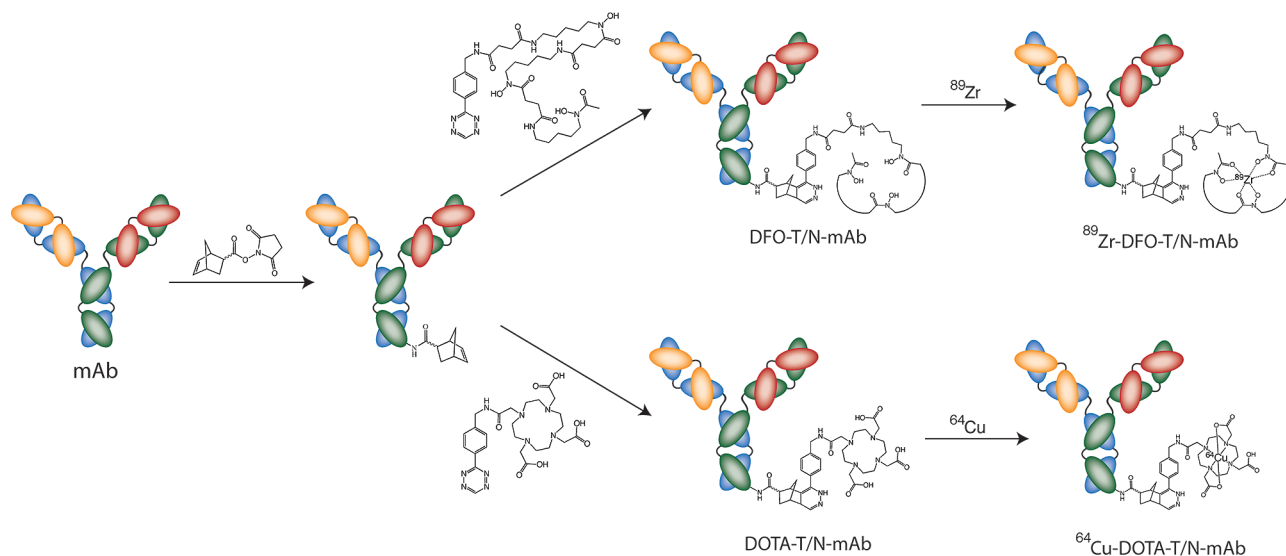


**Figure 2.** Schematic of a modular strategy for the construction of  $^{89}\text{Zr}$ - and  $^{64}\text{Cu}$ -modified antibody bioconjugates using the tetrazine-norbornene ligation.

yield [ $^{64}\text{Cu}$ ] $\text{CuCl}_2$  with an effective specific activity of 200–400  $\text{mCi}/\mu\text{g}$  (7.4–14.8  $\text{GBq}/\mu\text{g}$ ).<sup>50</sup>  $^{89}\text{Zr}$  was produced at Memorial Sloan-Kettering Cancer Center on an EBCO TR19/9 variable-beam energy cyclotron (EbcO Industries Inc., British Columbia, Canada) via the  $^{89}\text{Y}(p,n)^{89}\text{Zr}$  reaction and purified in accordance with previously reported methods to yield  $^{89}\text{Zr}$  with a specific activity of 5.28–13.43  $\text{mCi}/\mu\text{g}$  (195–497  $\text{MBq}/\mu\text{g}$ ).<sup>51</sup> All buffers used for  $^{64}\text{Cu}$  and  $^{89}\text{Zr}$  labeling were passed through Chelex resin before use. Activity measurements were made using a Capintec CRC-15R Dose Calibrator (Capintec, Ramsey, NJ). For accurate quantification of activities, experimental samples were counted for 1 min on a calibrated Perkin-Elmer (Waltham, MA) Automatic Wizard<sup>2</sup> Gamma Counter. Both  $^{64}\text{Cu}$  and  $^{89}\text{Zr}$  labeling reactions were monitored using silica-gel impregnated glass-fiber instant thin layer chromatography paper (Pall Corp., East Hills, NY) and analyzed on a Bioscan AR-2000 radio-TLC plate reader using Winscan Radio-TLC software (Bioscan Inc., Washington, DC). Human breast cancer cell lines BT-474 and MDA-MB-468 were obtained from the American Type Culture Collection (ATCC, Manassas, VA) and were grown by serial passage.

**Synthesis of 3-(4-Benzylamino)-1,2,4,5-tetrazine (Tz).** The protocol from Deveraj et al. was employed for the synthesis with slight modifications.<sup>24</sup> 4-(Aminomethyl)-benzonitrile hydrochloride (0.84 g, 0.005 mol) formamidine acetate (2.08 g, 0.02 mol), and elemental sulfur (0.16 g, 0.005 mol) were added to a dry, 50 mL round-bottom flask. Anhydrous hydrazine (2 mL) was then added to the flask, and the resultant orange reaction mixture was stirred for 20 h. After the allotted time, 1%  $\text{HCl}_{(\text{aq})}$  (50 mL) was slowly added to the reaction mixture, and the resultant solution was stirred for 10 min and subsequently filtered through a medium glass frit. The remaining orange solution was cooled in an ice bath to 0 °C, and a solution of 1.7 g of  $\text{NaNO}_2$  in 15 mL of water was then added dropwise to the reaction mixture. While still cooled in an ice bath, acetic acid (50 mL) was added slowly, and the reaction mixture immediately turned bright pink. After allowing this solution to warm to room temperature over the course of 3 h, the solvent was evaporated at 50 °C and 20 Torr on a rotary evaporator. The resultant red crude solids were dissolved in 250 mL of water with 0.1% TFA.

The aqueous solution was adsorbed onto a  $\text{C}_{18}$  column (Waters  $\text{C}_{18}$  Sep-Pak, Waters Corp., Milford, MA), washed with copious amounts of water, and eluted with acetonitrile. This bright pink, organic solution was evaporated to dryness, and the red crude was purified by flash chromatography (CombiFlash automated chromatography system, Teledyne Isco Inc., Lincoln, NE) using a gradient of 100%  $\text{CHCl}_3$  (0.01% TFA) from 0 to 4 min followed by 0:100 MeOH (0.01%TFA)/ $\text{CHCl}_3$  (0.01% TFA) to 30:70 (0.01%TFA)/ $\text{HCl}_3$  (0.01% TFA) over 16 min. After the removal of solvent, the pure product was obtained in 35% yield (0.33 g, 0.0018 mol).  $^1\text{H}$  NMR (500 MHz,  $\text{D}_2\text{O}$ ),  $\delta$ , ppm: 10.46 (s, 1H), 8.54 (d, 2H), 7.77 (d, 1H), 4.41 (s, 2H). ESI-MS: 188.1  $[\text{M}+\text{H}]^+$ . HPLC  $t_{\text{R}} = 7.1$  min.

**Synthesis of  $N^1$ -(5-(4-((1,2,4,5-Tetrazin-3-yl)benzyl)amino)-4-oxobutanamido)pentyl)- $N^1$ -hydroxy- $N^4$ -(5-( $N$ -hydroxy-4-((5-( $N$ -hydroxyacetamido)pentyl)amino)-4-oxobutanamido)pentyl)succinamide (Tz-DFO).** 3-(4-Benzylamino)-1,2,4,5-tetrazine (8 mg, 0.045 mmol) was dissolved in DMSO (3 mL), and diisopropylethylamine (16  $\mu\text{L}$ , 0.09 mmol) was added to this solution. After 15 min of stirring at RT, the pink DMSO solution was added to a second, premixed solution of  $N$ -succinyl-desferrioxamine B (60 mg, 0.09 mmol) and benzotriazole-1-yl-oxy-tris-(dimethylamino)-phosphonium hexafluorophosphate (BOP, 53 mg, 0.12 mmol) in DMSO (3 mL). The combined reaction was stirred overnight and subsequently purified via  $\text{C}_{18}$  cartridge (Waters  $\text{C}_{18}$  Sep-Pak, Waters Corp., Milford, MA) and semipreparative reverse-phase HPLC. The purified product was obtained in 50% yield (molecular weight = 852.9, 19 mg, 0.023 mmol).  $^1\text{H}$  NMR (500 MHz,  $\text{DMSO}-d_6$ ),  $\delta$ , ppm: 10.59 (s, 1H), 9.64 (s, 1H), 9.59 (s, 1H), 8.49 (m, 1H), 8.44 (d, 2H), 7.9–7.7 (m, 3H), 7.51 (d, 2H), 4.44 (d, 2H), 3.5–3.5 (m, 6H), 3.05–2.95 (m, 6H), 2.55 (t, 4H), 2.45–2.35 (m, 4H), 2.25 (t, 4H), 1.97 (s, 3H), 1.52–1.48 (m, 6H), 1.40–1.36 (m, 6H), 1.23–1.20 (m, 6H). ESI-MS: 831.5  $[\text{M}+\text{H}]^+$ , 853.6  $[\text{M}+\text{Na}]^+$ . HPLC  $t_{\text{R}} = 10.2$  min.

**Synthesis of 2,2',2''-(10-(2-((1,2,4,5-Tetrazin-3-yl)benzyl)amino)-2-oxoethyl)-1,4,7,10-tetraazacyclododecane-1,4,7-triyl)triacetic acid (Tz-DOTA).** 3-(4-Benzylamino)-1,2,4,5-tetrazine (20 mg, 0.12 mmol) was dissolved in PBS (5 mL, pH 8.5), and diisopropylethylamine (40  $\mu\text{L}$ , 0.24 mmol) was added

to this solution. This solution was then added to solid DOTA-NHS (50 mg, 0.065 mmol), and the resultant solution was stirred overnight at room temperature. The reaction was subsequently purified via C<sub>18</sub> cartridge (Waters C<sub>18</sub> Sep-Pak, Waters Corp., Milford, MA) and semipreparative reverse-phase HPLC. The purified product was obtained in 62% yield (molecular weight = 573.6, 23 mg, 0.04 mmol). <sup>1</sup>H NMR (500 MHz, DMSO-*d*<sub>6</sub>),  $\delta$ , ppm: 10.61 (s, 1H), 9.11 (br s, 1H), 8.50 (d, 2H), 7.62 (d, 2H), 4.50 (s, 2H), 4.42–4.38 (m, 4H), 3.65 (br s, 4H), 10.61 (s, 1H), 3.65–3.55 (m, 8H), 3.18–3.14 (m, 8H). ESI-MS: 574.5 [M+H]<sup>+</sup>, 596.1 [M+Na]<sup>+</sup>, 612.2 [M+K]<sup>+</sup>. HPLC *t*<sub>R</sub> = 8.1 min.

**Antibody Modification.** A protocol similar to that published by Devaraj et al. was employed for antibody modification.<sup>24</sup> 5-Norbornene-2-carboxylic acid (40 mg, 0.29 mmol) was incubated with 1.3 equiv of disuccinimidyl carbonate (100 mg, 0.39 mmol) and 1 equiv of pyridine (23 mg, 0.29 mmol) in dry acetonitrile (3 mL) for 2 h at room temperature. After 2 h, the solvent was removed via rotary evaporation, and the crude norbornene-succinimidyl ester product was recovered. Trastuzumab (purchased commercially as Herceptin, Genentech, San Francisco, CA) was purified using centrifugal filter units with a 30 000 molecular weight cutoff (Amicon Ultra 4 Centrifugal Filtration Units, Millipore Corp., Billerica, MA) and phosphate buffered saline (PBS, pH 7.4) to remove  $\alpha$ - $\alpha$ -trehalose dihydrate, L-histidine, and polysorbate 20 additives. After purification, the antibody was taken up in PBS pH 8.0. Subsequently, 300  $\mu$ L of antibody solution (150–250  $\mu$ M) were combined with 100  $\mu$ L PBS pH 8.0 and 1.5, 3, or 5 equiv of the crude norbornene-NHS ester in 10  $\mu$ L of either DMF or DMSO. The reaction was incubated at room temperature for 2 h, followed by centrifugal filtration to purify the resultant antibody conjugate.

To perform the chelator ligation, 100  $\mu$ L antibody solution (75–150  $\mu$ M, PBS pH 7.4) was combined with 200  $\mu$ L buffer (PBS pH 7.4) and a 10-fold molar excess of either Tz-DOTA or Tz-DFO in 10  $\mu$ L DMSO (molar excess calculated based on initial norbornene reaction stoichiometry). The reaction was incubated at RT for 5 h and subsequently purified using centrifugal filtration to yield the completed DOTA- and DFO-modified antibodies. The final bioconjugates were stored in PBS pH 7.4 at 4 °C.

**Labeling of DOTA-T/N-trastuzumab with <sup>64</sup>Cu.** DOTA-T/N-trastuzumab (0.2–0.3 mg) was added to 200  $\mu$ L labeling buffer (50 mM NH<sub>4</sub>OAc, pH 5.5, though 50 mM NaOAc, pH 5.5 also is sufficient). [<sup>64</sup>Cu]CuCl<sub>2</sub> (29.6–37 MBq, 800–1000  $\mu$ Ci) in approximately 1–3  $\mu$ L 0.1 M HCl were then added to the antibody solution, and the resultant solution was incubated at room temperature for 1 h. After 1 h, the reaction progress was assayed using ITLC with an eluent of 50 mM EDTA, pH 5. The resultant <sup>64</sup>Cu-DOTA-T/N-trastuzumab was purified using either size-exclusion chromatography (Sephadex G-25 M, PD-10 column, 30 kDa, GE Healthcare; dead volume = 2.5 mL, eluted with 200 mL fractions of PBS, pH 7.4) or centrifugal column filtration. The radiochemical purity of the final radiolabeled bioconjugate was assayed by radio-TLC and was found to be >99% in all preparations. In the ITLC experiments, <sup>64</sup>Cu-DOTA-T/N-trastuzumab remains at the baseline, while <sup>64</sup>Cu<sup>2+</sup> ions and [<sup>64</sup>Cu]Cu-EDTA elute with the solvent front.

**Labeling of DFO-T/N-trastuzumab with <sup>89</sup>Zr.** DFO-T/N-trastuzumab (0.2–0.3 mg) was added to 200  $\mu$ L buffer (PBS, pH 7.5). [<sup>89</sup>Zr]Zr-oxalate (29.6–37 MBq, 800–1000  $\mu$ Ci) in 1.0 M oxalic acid was adjusted to pH 7.2–8.5 with 1.0 M Na<sub>2</sub>CO<sub>3</sub>. After evolution of CO<sub>2</sub>(g) stops, the <sup>89</sup>Zr solution was added to the

antibody solution, and the resultant mixture was incubated at room temperature for 1 h. After 1 h, the reaction progress was assayed using ITLC with an eluent of 50 mM EDTA, pH 5. The resultant <sup>89</sup>Zr-DFO-T/N-trastuzumab was purified using either size-exclusion chromatography (Sephadex G-25 M, PD-10 column, 30 kDa, GE Healthcare; dead volume = 2.5 mL, eluted with 200 mL fractions of PBS, pH 7.4) or centrifugal column filtration. The radiochemical purity of the final radiolabeled bioconjugate was assayed by radio-TLC and was found to be >99% in all preparations. In the ITLC experiments, <sup>89</sup>Zr-DFO-T/N-trastuzumab remains at the baseline, while <sup>89</sup>Zr<sup>4+</sup> ions and [<sup>89</sup>Zr]-EDTA elute with the solvent front.

**Chelate Number.** The number of accessible DFO and DOTA chelates conjugated to the antibodies was measured by radio-metric isotopic dilution assays following methods similar to those described by Anderson et al. and Holland et al.<sup>34,42,52,53</sup> All experiments were performed in triplicate.

**Immunoreactivity.** The immunoreactivity of the <sup>64</sup>Cu-DOTA- and <sup>89</sup>Zr-DFO-T/N-trastuzumab bioconjugates was determined using specific radioactive cellular-binding assays following procedures derived from Lindmo et al.<sup>54,55</sup> To this end, BT-474 cells were suspended in microcentrifuge tubes at concentrations of 5.0, 4.0, 3.0, 2.5, 2.0, 1.5, and 1.0  $\times 10^6$  cells/mL in 500  $\mu$ L PBS (pH 7.4). Aliquots of either <sup>64</sup>Cu-DOTA- or <sup>89</sup>Zr-DFO-T/N-trastuzumab (50  $\mu$ L of a stock solution of 10  $\mu$ Ci in 10 mL of 1% bovine serum albumin in PBS pH 7.4) were added to each tube (*n* = 4; final volume: 550  $\mu$ L), and the samples were incubated on a mixer for 60 min at room temperature. The treated cells were then pelleted via centrifugation (3000 rpm for 5 min), resuspended, and washed twice with cold PBS before removing the supernatant and counting the activity associated with the cell pellet. The activity data were background-corrected and compared with the total number of counts in appropriate control samples. Immunoreactive fractions were determined by linear regression analysis of a plot of (total/bound) activity against (1/[normalized cell concentration]). No weighting was applied to the data, and data were obtained in triplicate.

**Stability Measurements.** The stability of the <sup>64</sup>Cu-DOTA- and <sup>89</sup>Zr-DFO-T/N-trastuzumab bioconjugates with respect to radiochemical purity and loss of radioactivity from the antibody was investigated *in vitro* by incubation of the antibodies in human serum for 48 h (<sup>64</sup>Cu) or 7 d (<sup>89</sup>Zr) at room temperature and 37 °C. The radiochemical purity of the antibodies was determined via radio-TLC with an eluent of 50 mM EDTA pH 5.0 (*vide supra*).

**Cell Culture.** Human breast cancer cell lines BT474 and MDA-MB-468 were obtained from the American Tissue Culture Collection (HTB-20 and HTB-132, respectively, ATCC, Bethesda, MD) and maintained in a 1:1 mixture of Dulbecco's Modified Eagle medium: F-12 medium, supplemented with 10% heat-inactivated fetal calf serum (Omega Scientific, Tarzana, Ca), 2.0 mM glutamine, nonessential amino acids, and 100 units/mL penicillin, and 100 units/mL streptomycin in a 37 °C environment containing 5% CO<sub>2</sub>. Cell lines were harvested and passaged weekly using a formulation of 0.25% trypsin/0.53 mM EDTA in Hank's Buffered Salt Solution without calcium and magnesium.

**Xenograft Models.** All experiments were performed under an Institutional Animal Care and Use Committee-approved protocol, and the experiments followed institutional guidelines for the proper and humane use of animals in research. Six- to eight-week-old Athymic nu/nu female mice (NCRNU-M) were obtained from Taconic Farms Incorporated (Hudson, NY). Animals were

housed in ventilated cages, were given food and water *ad libitum*, and were allowed to acclimatize for approximately 1 week prior to treatment. Prior to tumor inoculation, mice were subcutaneously implanted with 0.72 mg 60 day release  $17\beta$ -estradiol pellets (SE-121, Innovative Research of America, Sarasota, Florida) using a 10 gauge trocar. After several days, BT474 tumors were induced on the right shoulder by a subcutaneous injection of  $3.0 \times 10^6$  cells in a 100  $\mu$ L cell suspension of a 1:1 mixture of fresh media/BD Matrigel (BD Biosciences, Bedford, MA). MDA-MB-468 tumors were induced on the left shoulder by a subcutaneous injection of  $2.0 \times 10^6$  cells in the same manner (the number of cells injected was varied as described to compensate for cell growth rates and thus provide approximately the same tumor size at the time of radiopharmaceutical injection).

**Acute Biodistribution.** Acute *in vivo* biodistribution studies were performed in order to evaluate the uptake of the  $^{64}\text{Cu}$ -DOTA- and  $^{89}\text{Zr}$ -DFO-conjugated antibodies in mice bearing bilateral, subcutaneous BT-474 and MDA-MB-468 tumors (100–150  $\text{mm}^3$ , 4 weeks postinoculation). Mice were randomized before the study and were warmed gently with a heat lamp for 5 min before administration of  $^{64}\text{Cu}$ -DOTA-T/N-trastuzumab (0.74–1.11 MBq [20–30  $\mu\text{Ci}$ ] in 200  $\mu\text{L}$  0.9% sterile saline) or  $^{89}\text{Zr}$ -DFO-T/N-trastuzumab (0.56–0.74 MBq [15–20  $\mu\text{Ci}$ ] in 200  $\mu\text{L}$  0.9% sterile saline) via intravenous tail vein injection ( $t = 0$ ). Animals ( $n = 4$  per group) were euthanized by  $\text{CO}_2$ (g) asphyxiation at 6, 12, 24, 36, 48, and 72 h ( $^{64}\text{Cu}$ ) or 6, 24, 48, 72, 96, and 120 h ( $^{89}\text{Zr}$ ). After asphyxiation, 13 organs (including both tumors) were removed, rinsed in water, dried in air for 5 min, weighed, and counted in a gamma counter calibrated for either  $^{64}\text{Cu}$  or  $^{89}\text{Zr}$ . Counts were converted into activity using a calibration curve generated from known standards. Count data were background- and decay-corrected to the time of injection, and the percent injected dose per gram (%ID/g) for each tissue sample was calculated by normalization to the total activity injected.

**Small-Animal PET Imaging.** PET imaging experiments were conducted on either a microPET Focus 120 ( $^{89}\text{Zr}$ ) or a microPET R4 ( $^{64}\text{Cu}$ ) rodent scanner (Concorde Microsystems).<sup>56</sup> Mice bearing bilateral, subcutaneous BT-474 (right shoulder) and MDA-MB-468 (left shoulder) tumors (100–150  $\text{mm}^3$ , 4 weeks postinoculation) were administered  $^{64}\text{Cu}$ -DOTA-T/N-trastuzumab (11.1–12.9 MBq [300–345  $\mu\text{Ci}$ ] in 200  $\mu\text{L}$  0.9% sterile saline) or  $^{89}\text{Zr}$ -DFO-T/N-trastuzumab (10.7–11.8 MBq [290–320  $\mu\text{Ci}$ ] in 200  $\mu\text{L}$  0.9% sterile saline) via intravenous tail vein injection ( $t = 0$ ). Approximately 5 min prior to the acquisition of PET images, mice were anesthetized by inhalation of 2% isoflurane (Baxter Healthcare, Deerfield, IL)/oxygen gas mixture and placed on the scanner bed; anesthesia was maintained using 1% isoflurane/gas mixture. PET data for each mouse were recorded via static scans at various time points between 6 and 120 h. A minimum of 20 million coincident events were recorded for each scan, which lasted between 10 and 45 min. An energy window of 350–700 keV and a coincidence timing window of 6 ns were used. Data were sorted into 2D histograms by Fourier rebinning, and transverse images were reconstructed by filtered back-projection (FBP) into a  $128 \times 128 \times 63$  ( $0.72 \times 0.72 \times 1.3 \text{ mm}^3$ ) matrix. The image data were normalized to correct for nonuniformity of response of the PET, dead-time count losses, positron branching ratio, and physical decay to the time of injection, but no attenuation, scatter, or partial-volume averaging correction was applied. The counting rates in the reconstructed images were converted to activity concentrations (percentage

injected dose [%ID] per gram of tissue) by use of a system calibration factor derived from the imaging of a mouse-sized water-equivalent phantom containing  $^{64}\text{Cu}$  or  $^{89}\text{Zr}$ . Images were analyzed using *ASIPro VM* software (Concorde Microsystems).

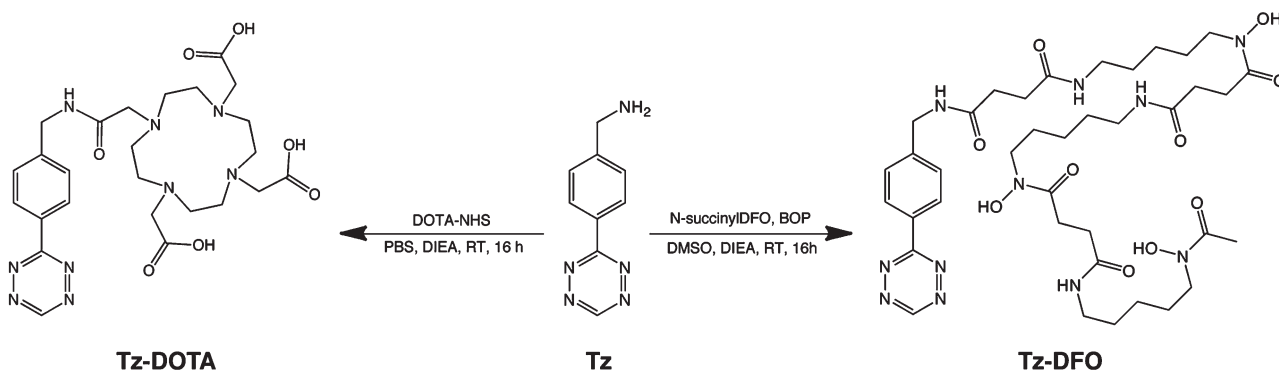
**Labeling Norbornene-Trastuzumab with [ $^{64}\text{Cu}$ ]-Tz-DOTA.** Tz-DOTA (5  $\mu\text{L}$  of 1 mM solution in DMSO) was added to labeling buffer (50 mM  $\text{NH}_4\text{OAc}$ , pH 5.5), and [ $^{64}\text{Cu}$ ]CuCl<sub>2</sub> (40.7–55.5 MBq [1100–1500  $\mu\text{Ci}$ ]) in 0.1 M HCl were added to the reaction mixture. The resultant solution was incubated for 1 h at 85 °C, followed by purification via C<sub>18</sub> cartridge (Waters C<sub>18</sub> Sep-Pak, Waters Corp., Milford, MA) and radiochemical purity analysis via analytical HPLC ( $t_{\text{R}} = 10$  min). The purified, radiolabeled [ $^{64}\text{Cu}$ ]-Tz-DOTA was then added to a solution of norbornene-modified trastuzumab (0.4 mg, initial reaction stoichiometry of 5:1 norbornene/mAb) in PBS pH 7.4. The reaction mixture was allowed to incubate at 37 °C for 3 h. After 3 h, the progress of the reaction was assayed with radio-TLC using an eluent of 50 mM EDTA pH 5.0, and the radiolabeled antibody was purified with centrifugal filtration using centrifugal filter units with a 30 000 molecular weight cutoff (Amicon Ultra 4 Centrifugal Filtration Units, Millipore Corp., Billerica, MA) and phosphate buffered saline (PBS, pH 7.4). The radiochemical purity of the final radiolabeled bioconjugate was assayed again by radio-TLC and was found to be >99% in all preparations. In the radio-TLC experiments,  $^{64}\text{Cu}$ -DOTA-T/N-trastuzumab remains at the baseline, while  $^{64}\text{Cu}^{2+}$  ions, [ $^{64}\text{Cu}$ ]Cu-Tz-DOTA, and [ $^{64}\text{Cu}$ ]Cu-EDTA elute with the solvent front.

**Statistical Analysis.** Data were analyzed by the unpaired, two-tailed Student's *t* test. Differences at the 95% confidence level ( $P < 0.05$ ) were considered to be statistically significant.

## RESULTS AND DISCUSSION

**Chemical Synthesis.** 3-(4-Benzylamino)-1,2,4,5-tetrazine (Tz) was successfully synthesized through the reaction of 4-(aminomethyl)-benzotrifluoride hydrochloride, formamidine acetate, and elemental sulfur to form a dihydrotetrazine intermediate ((4-(1,2-dihydro-1,2,4,5-tetrazin-3-yl)phenyl)methanamine), followed by oxidation with  $\text{NaNO}_2$  to form the aromatic tetrazine product. A method similar to that published by Devaraj et al. was employed; however, a number of small changes—for example, the use of 1%  $\text{HCl}_{(\text{aq})}$  rather than acetic acid in an intermediate step—were made and were found to considerably raise yields from the reported 20% to 35–40%. The product was characterized via UV–vis,  $^1\text{H}$  NMR,  $^{13}\text{C}$  NMR, and ESI-MS, and all data match that described in the original synthetic report.<sup>24</sup> Given the particularly promising nature of this cycloaddition reaction, the optimization of this synthesis was an important task. Tz was chosen as the particular tetrazine-based moiety for this line of experimentation due to its convenient, primary-amine coupling handle and its balance of reactivity and stability. To be sure, other tetrazine-based molecules with possible conjugation sites exist, but water instability (dimethyl 1,2,4,5-tetrazine-3,6-dicarboxylate), poor reactivity (1,2,4,5-tetrazine-3,6-diamine or 3,6-bis-(4-aminophenyl)-1,2,4,5-tetrazine), or instability (6-(6-(pyridin-2-yl)-1,2-dihydro-1,2,4,5-tetrazin-3-yl)pyridin-3-amine) render them unsuitable to the development of a modular system such as this.<sup>29,57–59</sup> Tz-DOTA and Tz-DFO (Scheme 1) were synthesized from Tz via simple peptide coupling reactions using the commercially available mono-NHS-ester of DOTA or *N*-succinyl-desferrioxamine B and benzotriazole-1-yl-oxy-tris-(dimethylamino)-phosphonium hexafluorophosphate (BOP), respectively.

Scheme 1. Synthetic Route to Tz-DOTA and Tz-DFO

Table 1. Chemical and Biological Characterization Data for  $^{64}\text{Cu}$ -DOTA-T/N- and  $^{89}\text{Zr}$ -DFO-T/N-trastuzumab Bioconjugates

radionuclide	chelator	initial Nor/mAb reaction stoichiometry	chelates/mAb <sup>a</sup>	specific activity (mCi/mg)	immunoreactive fraction <sup>b</sup>	stability <sup>c</sup>
$^{64}\text{Cu}$	DOTA	1.5	1.0 ± 0.2	3.2 ± 0.4	0.96 ± 0.05	>98%
		3	2.3 ± 0.4	3.1 ± 0.2	0.95 ± 0.03	>96%
		5	3.7 ± 0.7	5.3 ± 0.5	0.94 ± 0.02	>96%
$^{89}\text{Zr}$	DFO	1.5	1.1 ± 0.3	2.7 ± 0.2	0.96 ± 0.03	>98%
		3	2.2 ± 0.3	2.9 ± 0.3	0.96 ± 0.04	>98%
		5	3.8 ± 0.9	4.3 ± 0.4	0.93 ± 0.05	>97%

<sup>a</sup>  $n = 3$  for all experiments presented. <sup>b</sup> Determined prior to *in vivo* experimentation. <sup>c</sup> Calculated for incubation in human serum at 37 °C for 48 h (Cu) or 7 d (Zr).

Upon synthesis, both molecules were purified via reversed-phase HPLC and fully characterized by UV-vis,  $^1\text{H}$  NMR,  $^{13}\text{C}$  NMR, and ESI-MS. Importantly, Tz-DOTA exhibits high water solubility, but Tz-DFO does not. Consequently, DMSO was used as the stock solvent and delivery vehicle for both Tz-DOTA and Tz-DFO throughout the investigation in order to ensure that the antibodies in different branches of the modular pathway were exposed to exactly the same reaction conditions. Indeed, given the ease of synthesis of both Tz-DOTA and Tz-DFO, it is easy to envision the creation of a complete library of tetrazine-modified chelators—ranging from Tz-AmBaSar to Tz-HBED to Tz-DTPA—in order to maximize the utility and versatility of this modular construction strategy.

**Antibody Modification, Radiolabeling, and Characterization.** The radiolabeled trastuzumab bioconjugates were constructed via a modular three-step procedure (Figure 2). A common stock of norbornene-modified mAb was first produced via the room-temperature aqueous coupling of an NHS-ester of 5-norbornene-2-carboxylic acid with the exposed lysines of trastuzumab. After purification, the resultant norbornene-modified antibodies were then incubated for 5 h at room temperature with a 10-fold excess (based on norbornene loading) of the appropriate tetrazine-modified chelator—Tz-DOTA for  $^{64}\text{Cu}$  or Tz-DFO for  $^{89}\text{Zr}$ —and purified via centrifugal filtration or size exclusion chromatography. The bioconjugates were radiometalated with  $^{64}\text{Cu}$  or  $^{89}\text{Zr}$  at room temperature under either acidic (pH 5.5) or basic (pH 7.2–8.5) conditions, respectively. The crude radiochemical yields varied according to the initial norbornene loading of the antibody; however, after purification via centrifugal filtration, the  $^{64}\text{Cu}$ -DOTA- or  $^{89}\text{Zr}$ -DFO-T/N-trastuzumab conjugates were isolated with RCP >99% ( $n = 3$  for each

construct). The modification and radiolabeling strategy is simple, robust, and relatively rapid, and no antibody aggregation or precipitation issues were observed. Unlike other methods for the modification of mAbs with DOTA or DFO, overnight incubations, wide swings in buffer pH, and temperatures over room temperature are not required.<sup>60–64</sup> Importantly, we also observed that the tetrazine-norbornene ligation and subsequent radiolabeling proceeded almost identically whether performed the day of norbornene modification of the antibody or four weeks later (and likely after much longer periods of time, provided the antibody is stored at 4 °C). The radiolabeling of the DOTA- and DFO-modified trastuzumab conjugates is likewise robust, with the reaction providing similar yields with freshly prepared or four-week-old mAbs.

A number of chemical and *in vitro* tests were performed in order to characterize the chelator-modified and radiolabeled antibody constructs. Three different initial reaction stoichiometries of norbornene:mAb—1.5:1, 3:1, and 5:1—were employed to investigate the effect of different chelator loadings on the performance of the antibody. After the ligation of the variably norbornene-loaded antibodies with either Tz-DOTA or Tz-DFO, radiometric isotopic dilution experiments were performed in order to determine the number of accessible chelates on each antibody. The results, shown in Table 1, clearly illustrate that increasing initial loadings of norbornene result in higher numbers of chelates per antibody. Given the quantitative nature of the tetrazine/norbornene ligation and the proximity of the number of chelates per antibody to the initial modification stoichiometry in each case, calculating the loading of norbornenes per antibody was deemed unnecessary. The combined yield of the modification and ligation reactions is relatively consistent across all three

stoichiometries ( $\sim 40\text{--}60\%$ ), and the results are generally consistent with antibody ligations using tetrazine/dienophile pairs reported by Devaraj et al., Haun et al., and Rossin et al.<sup>23,28,29</sup> Just as importantly, the number of chelates per antibody is, within error, identical for both the DOTA-T/N-trastuzumab and DFO-T/N-trastuzumab conjugates, a critical facet for such a modular system. Not surprisingly, the varying chelate numbers also played a role in the specific activities obtained for each antibody. All of the antibody conjugates were labeled in high specific activity ( $>2.0$  mCi/mg). Interestingly, the specific activities of both the  $^{64}\text{Cu}$ -DOTA-T/N-trastuzumab and  $^{89}\text{Zr}$ -DFO-T/N-trastuzumab conjugates only roughly correlate with the number of chelates per antibody: those for  $^{64}\text{Cu}$ -DOTA-T/N-trastuzumab range from  $3.2 \pm 0.4$  mCi/mg to  $5.3 \pm 0.5$  mCi/mg, though the specific activities for bioconjugates with initial nor/mAb ratios of 1.5:1 and 3:1 are within error of each other. Similarly, the specific activities of the  $^{89}\text{Zr}$ -DFO-T/N-trastuzumab conjugates range from  $2.7 \pm 0.2$  mCi/mg to  $4.3 \pm 0.4$  mCi/mg, but again, the specific activities of the two conjugates with fewer DFO/mAb are statistically identical. Given the different specific activities of the original radiometals, comparisons between the specific activities of the two types of construct have little merit; however, the specific activities obtained in this investigation are consistent with those reported for other  $^{64}\text{Cu}$ -DOTA-based and  $^{89}\text{Zr}$ -DFO-based antibody bioconjugates in the literature.<sup>6,10,34,42,45</sup>

The immunoreactive fractions of the  $^{64}\text{Cu}$ -DOTA- and  $^{89}\text{Zr}$ -DFO-conjugates were determined via specific *in vitro* cellular association assays using the HER2/*neu* positive BT-474 breast cancer cell line.<sup>54</sup> Regardless of the number of chelates per antibody, all six conjugates exhibited immunoreactive fractions greater than 0.93 ( $n = 3$  for each radiolabeled antibody). Blocking experiments performed with the addition of a vast excess ( $>500$ -fold) of unlabeled trastuzumab showed virtually no radioactive antibody binding and thus demonstrated the specificity of the  $^{64}\text{Cu}$ -DOTA- and  $^{89}\text{Zr}$ -DFO-T/N-trastuzumab. To assay the stability of radiolabeled bioconjugates, the  $^{64}\text{Cu}$ -DOTA- and  $^{89}\text{Zr}$ -DFO-T/N-trastuzumab formulations were incubated in human serum for 48 h and 7 d, respectively. Radio-TLC with an eluent of 50 mM EDTA (pH 5.0) illustrated that both sets of conjugates were  $>96\%$  stable after the incubation period in all cases (Table 1).

**Acute Biodistribution Studies.** Acute biodistribution experiments and small animal PET imaging were performed in order to assay the *in vivo* efficacy of the  $^{64}\text{Cu}$  and  $^{89}\text{Zr}$ -bioconjugates. For all *in vivo* investigations, the trastuzumab bioconjugates with an initial nor/mAb stoichiometry of 5:1 were chosen, though similar results would be expected for all three ratios given the uniformly high immunoreactivity, stability, and specific activity observed in all of the constructs. In the biodistribution experiment, nude mice bearing bilateral BT-474 (HER2-positive) and MDA-MB-468 (HER2-negative) were injected via tail vein with either  $^{64}\text{Cu}$ -DOTA-T/N-trastuzumab ( $0.74\text{--}1.11$  MBq [ $20\text{--}30$   $\mu\text{Ci}$ ] in 200  $\mu\text{L}$  0.9% sterile saline, specific activity: 5.1 mCi/mg) or  $^{89}\text{Zr}$ -DFO-T/N-trastuzumab ( $0.56\text{--}0.74$  MBq [ $15\text{--}20$   $\mu\text{Ci}$ ] in 200  $\mu\text{L}$  0.9% sterile saline, specific activity: 4.7 mCi/mg). Animals ( $n = 4$  for each time point) were euthanized by  $\text{CO}_2$ (g) asphyxiation at 6, 12, 24, 36, 48, and 72 h ( $^{64}\text{Cu}$ ) or 6, 24, 48, 72, 96, and 120 h ( $^{89}\text{Zr}$ ). The organs (including tumors) of each animal were harvested and weighed, the amount of activity in each was counted on a gamma counter, and the %ID/g for each organ was calculated.

**Table 2. Biodistribution Data of  $^{64}\text{Cu}$ -DOTA-T/N-trastuzumab versus Time in Mice Bearing Bilateral s.c. BT-474 (HER2-positive) and MDA-MB-468 (HER2-negative) Xenografts ( $n = 4$  for Each Time Point)**

	6 h	12 h	24 h	48 h	72 h
blood	19.2 $\pm$ 5.2	16.2 $\pm$ 4.1	10.5 $\pm$ 3.6	11.2 $\pm$ 1.6	11.8 $\pm$ 1.3
HER2+ tumor	10.4 $\pm$ 4.6	23.9 $\pm$ 4.6	26.1 $\pm$ 4.8	44.0 $\pm$ 7.7	55.1 $\pm$ 2.3
HER2- tumor	6.2 $\pm$ 1.1	8.6 $\pm$ 2.7	9.0 $\pm$ 0.9	8.7 $\pm$ 2.5	11.7 $\pm$ 1.3
heart	4.9 $\pm$ 1.1	6.7 $\pm$ 2.7	4.3 $\pm$ 0.8	4.3 $\pm$ 1.2	5.7 $\pm$ 3.1
lungs	12.2 $\pm$ 1.2	9.5 $\pm$ 1.5	6.4 $\pm$ 2.3	8.0 $\pm$ 1.3	9.5 $\pm$ 0.4
liver	11.5 $\pm$ 2.0	10.1 $\pm$ 0.4	9.7 $\pm$ 1.3	6.4 $\pm$ 0.2	8.1 $\pm$ 0.9
spleen	11.1 $\pm$ 5.5	10.1 $\pm$ 1.4	10.6 $\pm$ 2.3	5.7 $\pm$ 0.4	6.9 $\pm$ 1.4
stomach	1.9 $\pm$ 0.7	1.0 $\pm$ 0.4	2.4 $\pm$ 0.3	1.3 $\pm$ 0.3	1.8 $\pm$ 0.2
sm intestine	3.5 $\pm$ 1.5	2.1 $\pm$ 0.3	3.5 $\pm$ 1.6	2.2 $\pm$ 0.1	2.6 $\pm$ 0.1
lg intestine	2.0 $\pm$ 0.3	1.7 $\pm$ 0.1	3.1 $\pm$ 1.7	1.4 $\pm$ 0.3	2.0 $\pm$ 0.4
kidney	5.5 $\pm$ 0.9	4.9 $\pm$ 1.0	2.9 $\pm$ 1.6	4.0 $\pm$ 0.4	4.5 $\pm$ 0.4
muscle	0.6 $\pm$ 0.2	0.7 $\pm$ 0.4	0.6 $\pm$ 0.3	1.0 $\pm$ 0.2	0.8 $\pm$ 0.1
bone	3.1 $\pm$ 2.7	1.4 $\pm$ 0.1	3.6 $\pm$ 0.4	1.1 $\pm$ 0.2	2.6 $\pm$ 1.1

In the  $^{64}\text{Cu}$ -DOTA-T/N-trastuzumab biodistribution experiment (Table 2), high specific uptake is observed in the HER2-positive BT-474 tumor, with the %ID/g increasing from  $10.4 \pm 4.6$  at 6 h to  $55.1 \pm 2.3$  at 72 h (tumor/muscle ratios of  $17.3 \pm 7.1$  and  $68.8 \pm 8.0$ , respectively). By comparison, far lower levels of  $^{64}\text{Cu}$ -DOTA-T/N-trastuzumab uptake were seen in the HER2-negative MDA-MB-468 tumors. As expected, over the course of the experiment a concomitant decrease in the %ID/g in the blood (from  $19.2 \pm 5.2$  at 6 h to  $11.8 \pm 1.3$  at 72 h) also occurred. The organs with the highest background uptake were the lungs, liver, and spleen, though the uptake in these organs was at its highest point at 6 h, and by 72 h, the tumor/organ ratios for each of these organs were  $5.8 \pm 0.3$ ,  $6.8 \pm 0.8$ , and  $8.0 \pm 1.6$ , respectively (see Supporting Information for complete table of tumor/organ ratios). Low levels of uptake were observed in the heart, stomach, small intestine, large intestine, kidney, muscle, and bone. Taken together, these results plainly indicate that  $^{64}\text{Cu}$ -DOTA-T/N-trastuzumab is an effective imaging agent for the delineation of the HER2-positive BT-474 xenografts. Perhaps just as importantly, these results are consistent with those previously reported for  $^{64}\text{Cu}$ -DOTA-T/N-trastuzumab conjugates, though the literature investigation used HER2-positive and HER2-negative non-small cell lung cancer cell lines.<sup>65</sup> Interestingly, far lower background liver uptake was observed in our study, and while comparisons between different tumor models systems may bear some risks, this discrepancy suggests a lower rate of  $^{64}\text{Cu}$  decomplexation in our system.

Similarly positive results were observed in the  $^{89}\text{Zr}$ -DFO-T/N-trastuzumab biodistribution experiments (Table 3). Initially very high blood activity levels decreased over the course of the experiment, from  $42.2 \pm 8.8\%$ ID/g at 6 h to  $18.2 \pm 3.3\%$ ID/g at 120 h. More importantly, high specific uptake was observed in the HER2-positive BT474 tumors, peaking at over  $75\%$ ID/g at 72 h postinjection (tumor to muscle ratio:  $34.1 \pm 12.7$ ). In contrast, the uptake in the HER2-negative MDA-MB-468 tumors was significantly lower, starting at  $11.2 \pm 5.8\%$ ID/g at 6 h and peaking at 120 h at  $17.6 \pm 3.9\%$ ID/g. Highest background uptake was observed in the lungs, liver, spleen, and kidney, with uptake values ranging from 7 to  $17\%$ ID/g and typically decreasing over the course of the experiment. Maximum tumor to organ

**Table 3. Biodistribution Data of  $^{89}\text{Zr}$ -DFO-T/N-trastuzumab versus Time in Mice Bearing Bilateral s.c. BT-474 (HER2-positive) and MDA-MB-468 (HER2-negative) Xenografts ( $n = 4$  for Each Time Point)**

	6 h	24 h	48 h	72 h	96 h	120 h
blood	42.2 ± 8.8	37.4 ± 3.4	24.1 ± 6.1	24.1 ± 8.2	20.2 ± 2.1	18.2 ± 3.3
HER2+ tumor	22.9 ± 6.6	48.6 ± 6.9	64.0 ± 6.8	75.1 ± 7.6	72.2 ± 7.9	69.8 ± 3.9
HER2- tumor	11.2 ± 5.0	13.4 ± 4.1	14.5 ± 8.8	16.8 ± 2.7	16.7 ± 6.8	17.6 ± 1.7
heart	24.1 ± 5.7	17.7 ± 6.9	6.0 ± 3.2	9.6 ± 3.8	8.5 ± 3.2	10.4 ± 0.9
lungs	15.5 ± 2.4	15.8 ± 5.4	10.5 ± 4.6	11.9 ± 4.8	13.8 ± 8.1	12.9 ± 3.2
liver	24.2 ± 5.0	17.6 ± 4.7	16.0 ± 6.5	15.8 ± 1.4	12.8 ± 2.7	13.5 ± 7.3
spleen	11.3 ± 1.2	14.2 ± 5.3	15.0 ± 5.1	14.9 ± 5.2	12.6 ± 6.5	10.8 ± 5.3
stomach	6.7 ± 1.4	3.1 ± 0.2	2.5 ± 0.7	2.0 ± 0.5	1.9 ± 0.4	1.8 ± 0.3
small intestine	8.4 ± 1.7	6.3 ± 0.3	7.9 ± 2.9	4.8 ± 1.1	3.8 ± 0.9	4.4 ± 0.8
large intestine	4.5 ± 1.0	2.1 ± 0.6	1.7 ± 0.2	2.3 ± 0.9	1.0 ± 0.3	1.4 ± 0.5
kidney	15.9 ± 5.4	13.3 ± 1.2	7.0 ± 1.3	11.6 ± 2.6	10.2 ± 0.3	8.7 ± 2.9
muscle	2.2 ± 0.6	2.3 ± 0.2	1.6 ± 0.5	2.2 ± 0.4	2.2 ± 0.2	2.5 ± 0.2
bone	12.1 ± 0.8	13.2 ± 2.4	14.6 ± 3.8	15.2 ± 1.9	14.7 ± 3.1	15.1 ± 1.5

ratios for the lungs, liver, spleen, and kidney were  $6.2 \pm 2.6$  (72 h),  $5.6 \pm 1.3$  (96 h),  $6.6 \pm 3.2$  (120 h),  $9.8 \pm 3.4$  (72 h), respectively (see Supporting Information for complete table of complete tumor/organ ratios). As in the case of  $^{64}\text{Cu}$ -DOTA-T/N-trastuzumab, after the earliest time points, only low levels of uptake were detected in the stomach, small intestine, large intestine, and muscle. Interestingly, distinct bone uptake is also observed, with %ID/g values ranging from  $12.1 \pm 0.8$  at 6 h to  $15.2 \pm 1.9$  at 72 h. This is certainly not a surprise, for residual bone uptake of  $^{89}\text{Zr}$  has been reported on a number of occasions, and a recently published by Abou et al. has shown that bone uptake is the *in vivo* fate of a number of species of  $^{89}\text{Zr}$ , including [ $^{89}\text{Zr}$ ]Zr-oxalate, [ $^{89}\text{Zr}$ ]Zr-chloride, [ $^{89}\text{Zr}$ ]Zr-citrate.<sup>34,42,66</sup> While a full discussion of the metabolic fate of  $^{89}\text{Zr}$ -DFO-T/N-trastuzumab or  $^{89}\text{Zr}$ -DFO is, of course, out of the scope of this work, it is interesting to note that the bone uptake does not increase dramatically over the course of the experiment, suggesting that the majority of  $^{89}\text{Zr}$  deposition in the bone occurs very soon after injection.

Overall, these results are generally consistent with those previously reported for  $^{89}\text{Zr}$ -trastuzumab bioconjugates by Munnink et al. and Holland et al.<sup>42,43</sup> No other data have been published on the uptake of  $^{89}\text{Zr}$ -trastuzumab in HER2-negative MDA-MB-468 tumors; however, the uptake value obtained at 24 h in this study ( $13.4 \pm 4.1\%$ ID/g) is remarkably similar to the value obtained at the same time point in the blocking experiment (200  $\mu\text{g}$  additional unlabeled trastuzumab) performed by Holland et al. with BT-474 cells:  $13.5 \pm 4.8\%$ ID/g. While this latter experiment is not, of course, directly comparable, it does help establish a baseline for the nonspecific tumor uptake of radiolabeled antibody.

Overall, two key differences are evident upon comparing the biodistribution data obtained with  $^{89}\text{Zr}$ -DFO-T/N-trastuzumab and  $^{64}\text{Cu}$ -DOTA-T/N-trastuzumab. The first, increased bone uptake in the  $^{89}\text{Zr}$ -DFO-T/N-trastuzumab experiment, is easily explained: free  $^{89}\text{Zr}^{4+}$  is a bone-seeking radiometal, while free  $^{64}\text{Cu}^{2+}$  has not been shown to accumulate in bone. Second, the HER2-specific tumor uptake and background signal (including initial blood levels) are higher in the  $^{89}\text{Zr}$ -DFO-T/N-trastuzumab biodistribution than at the corresponding time points in the  $^{64}\text{Cu}$ -DOTA-T/N-trastuzumab experiment. For example, at 6 h, the blood levels for  $^{89}\text{Zr}$ -DFO-T/N-trastuzumab are

$42.2 \pm 8.8\%$ ID/g, while they are  $19.2 \pm 5.2\%$ ID/g for  $^{64}\text{Cu}$ -DOTA-T/N-trastuzumab. Later, at 48 h, the uptake in the HER2-positive BT-474 tumor for  $^{89}\text{Zr}$ -DFO-T/N-trastuzumab is  $72.2 \pm 7.9\%$ ID/g, while for  $^{64}\text{Cu}$ -DOTA-T/N-trastuzumab, it is  $44.0 \pm 7.7\%$ ID/g. Moreover, at 48 h, the liver uptake of  $^{89}\text{Zr}$ -DFO-T/N-trastuzumab stands at  $12.8 \pm 2.7\%$ ID/g, while it is  $6.4 \pm 0.2\%$ ID/g for  $^{64}\text{Cu}$ -DOTA-T/N-trastuzumab at the same time point. It is possible that these variations in background uptake result from differences in the metabolism of the  $^{89}\text{Zr}$ -DFO- and  $^{64}\text{Cu}$ -DOTA-modified antibodies. The increase in HER2-specific uptake of the  $^{89}\text{Zr}$ -DFO-T/N-trastuzumab is somewhat more puzzling, though these data are consistent with that obtained in other investigations of  $^{64}\text{Cu}$ - and  $^{89}\text{Zr}$ -trastuzumab.<sup>42,65</sup> In the case of small peptides, it has been previously reported that the identity of the radiometal may play a role in the uptake of otherwise identical radiopharmaceuticals;<sup>67</sup> however, given the vast size of antibodies, it is far less likely that the identity of the radiometal would exert as strong an influence in this case. Experiments are currently underway to further elucidate the origins of the differences between the pharmacodynamics of two conjugates.

Despite these differences, the biodistribution data plainly illustrate that both radiolabeled constructs are selectively and significantly taken up in the HER2-positive tumors. In addition, and perhaps more important in light of the goals of the investigation, the overall trends observed in uptake and tumor/organ ratio are strikingly similar in the two experiments.

**Small Animal PET Imaging.** Small animal PET imaging experiments were performed in order to further evaluate the *in vivo* behavior of the two radiometalated bioconjugates. In each case, nude mice ( $n = 5$  for each construct) bearing bilateral BT-474 (HER2-positive) and MDA-MB-468 (HER2-negative) xenografts were injected via tail vein with either  $^{64}\text{Cu}$ -DOTA-T/N-trastuzumab (11.1–12.9 MBq [300–345  $\mu\text{Ci}$ ]) or  $^{89}\text{Zr}$ -DFO-T/N-trastuzumab (10.7–11.8 MBq [290–320  $\mu\text{Ci}$ ]). The animals were subsequently imaged periodically from injection ( $t = 0$  h) to 48 h ( $^{64}\text{Cu}$ ) or 120 h ( $^{89}\text{Zr}$ ). The results clearly indicate that both constructs are taken up significantly and selectively in the HER2-positive BT-474 tumors (shown in Figures 3 and 4). In the case of  $^{64}\text{Cu}$ -DOTA-T/N-trastuzumab, high blood pool activity and some background uptake are evident at the early time points, but over the course of the experiment, the



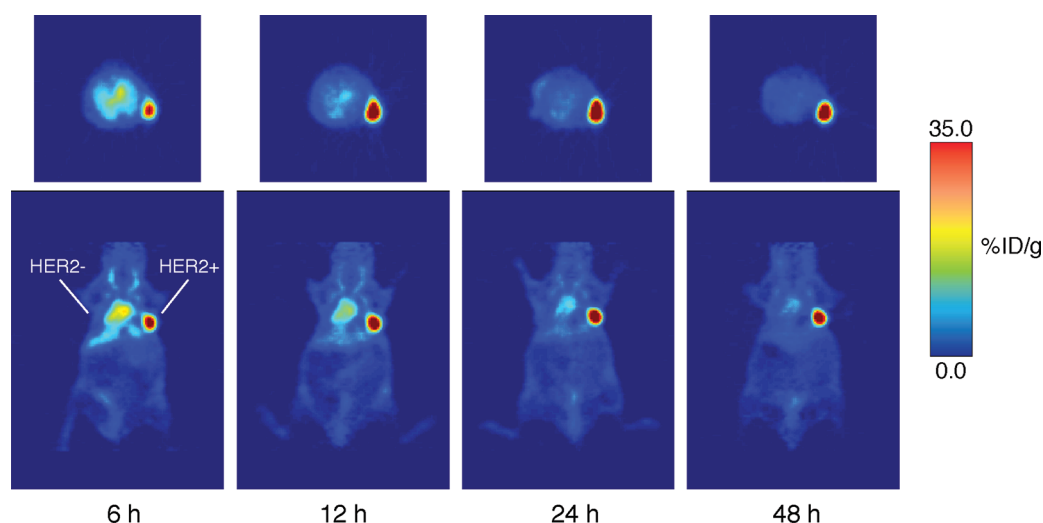


**Figure 3.** PET images of  $^{64}\text{Cu}$ -DOTA-T/N-trastuzumab (11.1–12.9 MBq [300–345  $\mu\text{Ci}$ ] in 200  $\mu\text{L}$  0.9% sterile saline) in mice bearing bilateral BT-474 (HER2-positive, right shoulder) and MDA-MB-468 (HER2-negative, left shoulder) tumors between 6 and 48 h postinjection. The transverse (top) and coronal (bottom) planar images intersect the center of the tumors.

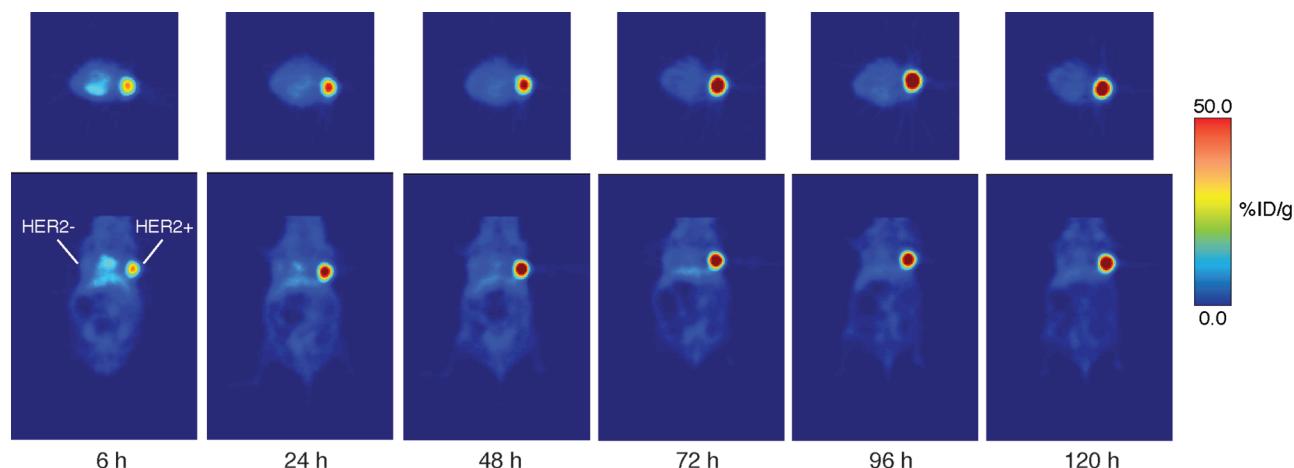


**Figure 4.** PET images of  $^{89}\text{Zr}$ -DFO-T/N-trastuzumab (10.7–11.8 MBq [290–320  $\mu\text{Ci}$ ] in 200  $\mu\text{L}$  0.9% sterile saline) in mice bearing bilateral BT-474 (HER2-positive, right shoulder) and MDA-MB-468 (HER2-negative, left shoulder) tumors between 6 and 120 h postinjection. The transverse (top) and coronal (bottom) planar images intersect the center of the tumors.

signal in the BT-474 tumor increases significantly to a point at which it is easily the most intense feature in the PET image. Similarly, for  $^{89}\text{Zr}$ -DFO-T/N-trastuzumab, some blood pool activity is evident at the earliest time point, but the tumor uptake increases steadily in the subsequent time points along with a concomitant decrease in any background activity. The images produced by the two conjugates are very similar, a result that is consistent with the sum of the data collected in this investigation. In each case, very little background uptake is evident in either the HER2-negative MDA-MB-468 tumor or other organs. The only significant differences, as in the biodistribution experiments, are enhanced tumor and background uptake in the  $^{89}\text{Zr}$ -DFO-T/N-trastuzumab images compared to those from  $^{64}\text{Cu}$ -DOTA-T/N-trastuzumab and slight bone uptake of the former construct. The bone uptake is not evident in the images displayed in Figure 5 but can be spotted (though faint) in a maximum intensity projection (see Supporting Information). Just as important as the imaging similarities between the two constructs in this study, the images

obtained here are consistent with those reported for other  $^{89}\text{Zr}$ - and  $^{64}\text{Cu}$ -trastuzumab radioagents in the literature.

**Radiolabeling Trastuzumab with a Two-Step Ligation Strategy.** The modular strategy described to this point comprises three simple steps: norbornene modification, tetrazine-chelator ligation, and radiometalation. However, the versatility of the tetrazine-norbornene ligation makes an alternate route possible as well: a two-step procedure in which a norbornene-modified antibody is reacted with a radiometalated, chelator-modified tetrazine (Figure 5). Indeed, similar ligations of dienophiles with radiolabeled tetrazines have already been employed with success with  $^{18}\text{F}$  and  $^{111}\text{In}$ , though in these cases, a transcyclooctene dienophile was employed rather than a norbornene.<sup>29–31</sup> To demonstrate the feasibility of such a strategy with PET radiometals, Tz-DOTA (5 nmol) was radiolabeled with  $^{64}\text{Cu}$  (1.1–1.5 mCi) in 50 mM  $\text{NH}_4\text{OAc}$  pH 5.5 via incubation at 85  $^\circ\text{C}$  for 1 h ( $n = 3$  trials). After the 1 h incubation, the labeling reaction was purified via radio-HPLC, and the product was obtained in an uncorrected

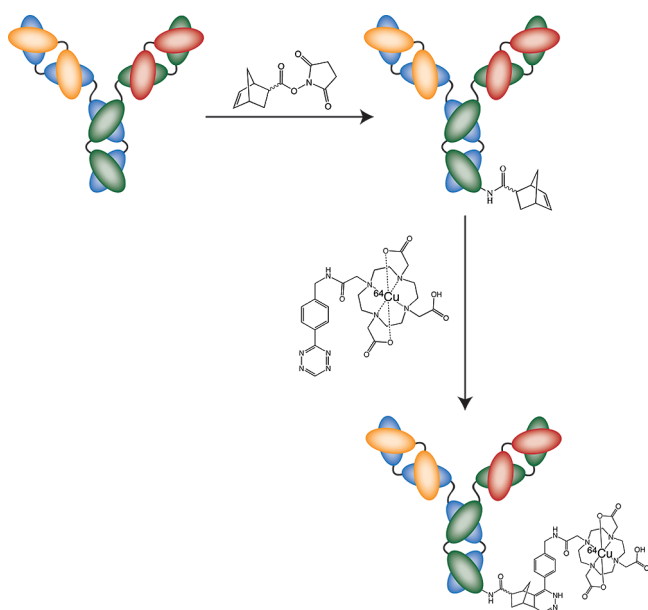


**Figure 5.** Schematic of the two-step radiolabeling strategy based on the ligation of norbornene-modified antibody and  $^{64}\text{Cu}$ -labeled Tz-DOTA.

radiochemical yield of  $80 \pm 3\%$  with greater than 99% radiochemical purity and a specific activity of  $160 \pm 5 \text{ mCi}/\mu\text{mol}$ . Subsequently, this  $^{64}\text{Cu}$ -Tz-DOTA was incubated with norbornene-modified trastuzumab (0.4 mg, 1.3 nmol, initial norbornene/mAb stoichiometry of 5:1) in PBS pH 7.4 (200  $\mu\text{L}$ ) at 37  $^{\circ}\text{C}$ . The progress of the reaction was monitored with radio-TLC, and after 3 h, the reaction was gauged to have reached completion. After purification via centrifugal filtration, the completed  $^{64}\text{Cu}$ -DOTA-T/N-trastuzumab conjugate was isolated in  $\sim 75\%$  radiochemical yield and in  $>99\%$  radiochemical purity with a specific activity of  $1.0 \pm 0.4 \text{ mCi}/\text{mg}$ . Granted, this specific activity is somewhat lower than that obtained with the three-step method; however, further optimization, though outside of the scope of the work at hand, could no doubt raise this specific activity to levels on par with that achieved with the three-step strategy.

Ultimately, it is our belief that the three-step method is preferable as a modular strategy for radiolabeling antibodies. This method holds the key advantage of only involving a single and relatively rapid radiochemical step, thereby minimizing the amount of radiochemistry needed for the creation of the bioconjugates while simultaneously maximizing specific activities. However, it is clear from the work currently in the literature—particularly that of Devaraj et al. and Rossin et al.—that the two-step method holds significant potential as a strategy for pretargeted antibody or peptide imaging.<sup>23,24,27–29,31</sup> In this application, a dienophile-modified biomolecule is first injected into a tumor-bearing animal and is permitted time to achieve its optimal biodistribution. Subsequently, a fluorophore- or radionuclide-modified tetrazine moiety is injected into the same animal and, due to the bioorthogonal nature of the tetrazine-dienophile ligation, could selectively react with the dienophile-modified biomolecule, resulting in specific localization of the marker. Indeed, both the optical and nuclear pretargeting strategies have shown very promising results. It is important to note, though, that the pretargeting systems described in the literature employ more reactive, less stable trans-cyclooctene

dienophiles instead of the more stable, less reactive norbornene dienophile used in this study. Experiments are currently underway toward the creation of a pretargeting system for positron-emitting radiometals employing more reactive dienophiles.

## CONCLUSION

In summary, herein we report the development of a modular system for the radiometalation of antibodies using the inverse electron demand Diels–Alder cycloaddition between tetrazine and norbornene. The strategy involves three facile, rapid, and biocompatible steps: modification of an antibody with norbornene, ligation of a chelator-modified tetrazine, and radiometalation. In this proof of concept investigation, the methodology was employed to create bioconjugates of the HER2-specific antibody trastuzumab bearing the positron-emitting radiometals  $^{64}\text{Cu}$  and  $^{89}\text{Zr}$  in high radiochemical purity and specific activity. For a given initial loading of norbornene, the DOTA- and DFO-modified constructs were shown to have identical numbers of chelates per antibody, and all of the radiolabeled  $^{64}\text{Cu}$ -DOTA- and  $^{89}\text{Zr}$ -DFO-bioconjugates displayed high serum stability and immunoreactivity. Finally, both radiolabeled bioconjugates were used in *in vivo* biodistribution and PET imaging studies with mice bearing HER2-positive (BT-474) and HER2-negative (MDA-MB-468) breast cancer xenografts. Both antibody constructs were shown to have significant and specific uptake in the HER2-positive tumor with low uptake in the HER2-negative tumor and other tissues.

This strategy does not necessarily offer a significant improvement in facility compared to popular DOTA-NHS or DFO-NCS antibody modification protocols; more importantly, however, it creates a modular platform in which a common, covalently modified antibody can be modified with a wide variety of chelators and radiometals. Given that different radiometals often require different chelators—and thus the use and optimization of different modification pathways—this methodology could no doubt aid in the rapid and robust construction of diverse radiopharmaceuticals from a single antibody stock. Further, this modular system could facilitate the creation of meaningful comparisons between bioconjugates labeled with different radiometals: as we have shown, because the chelator-modified antibodies are synthesized using identical ligation conditions, the immunoreactivity and chelator/antibody ratios of the resultant bioconjugates are likewise nearly identical regardless of the identity of the tetrazine–chelator pair.

Ultimately, therefore, this modular methodology has the potential not only to significantly aid in the synthesis and development of new radiometalated bioconjugates for PET, SPECT, and radiotherapy, but also to advance cross-pollination and constructive comparisons between radiopharmaceuticals employing diverse metallic radionuclides.

## ASSOCIATED CONTENT

**S Supporting Information.** Tables of tumor to muscle uptake ratios from  $^{89}\text{Zr}$ -DFO-T/N-trastuzumab and  $^{64}\text{Cu}$ -DOTA-T/N-trastuzumab biodistribution experiments and maximum intensity projection PET image of  $^{89}\text{Zr}$ -DFO-T/N-trastuzumab indicating residual bone uptake. This material is available free of charge via the Internet at <http://pubs.acs.org>.

## AUTHOR INFORMATION

## Corresponding Author

\*Phone: 1-646-888-3039. Fax: 1-646-888-3059. E-mail: lewisj2@mskcc.org.

## ACKNOWLEDGMENT

The authors thank Dr. Jason P. Holland for insight and helpful conversations, Valerie Longo for aid with animal imaging experiments, Nicholas Ramos for aid in the purification of  $^{89}\text{Zr}$ , and Alexander Veach for technical assistance. Services provided by the MSKCC Small-Animal Imaging Core Facility were supported in part by NIH grants R24 CA83084 and P30 CA08748. The authors also thank the NIH (Award 1F32CA1440138-01, BMZ; Award R01EB010011, RW) and the DOE (Award DE-SC0002184, JSL) for their generous funding.

## REFERENCES

- (1) van Dongen, G. A. M. S., Visser, G. W. M., Lub-de Hooge, M. N., de Vries, E. G., and Perk, L. R. (2007) Immuno-PET: a navigator in monoclonal antibody development and applications. *Oncologist* 12, 1379–1389.
- (2) Wu, A. M. (2009) Antibodies and antimatter: The resurgence of immuno-PET. *J. Nucl. Med.* 50, 2–5.
- (3) Zalutsky, M. R., and Lewis, J. S. (2003) Radiolabeled antibodies for tumor imaging and therapy. *Handb. Radiopharm.* 685–714.
- (4) Verel, I., Visser, G. W. M., Vosjan, M. J. W. D., Finn, R., Boellaard, R., and Van Dongen, G. A. M. S. (2004) High-quality 124I-labelled monoclonal antibodies for use as PET scouting agents prior to 131I-radioimmunotherapy. *Eur. J. Nucl. Med. Mol. Imaging* 31, 1645–1652.
- (5) Anderson, C. J., and Welch, M. J. (1999) Radiometal-labeled agents (non-technetium) for diagnostic imaging. *Chem. Rev.* 99, 2219–2234.
- (6) Wadas, T. J., Wong, E. H., Weisman, G. R., and Anderson, C. J. (2010) Coordinating radiometals of copper, gallium, indium, yttrium, and zirconium for PET and SPECT imaging of disease. *Chem. Rev.* 110, 2858–2902.
- (7) Nayak, T. K., and Brechbiel, M. W. (2009) Radioimmunoimaging with longer-lived positron-emitting radionuclides: potentials and challenges. *Bioconjugate Chem.* 20, 825–841.
- (8) Divgi, C. R., Pandit-Taskar, N., Jungbluth, A. A., Reuter, V. E., Gönen, M., Ruan, S., Pierre, C., Nagel, A., Pryma, D. A., Humm, J., Larson, S. M., Old, L. J., and Russo, P. (2007) Preoperative characterization of clear-cell renal carcinoma using iodine-124-labelled antibody chimeric G250 (124I-cG250) and PET in patients with renal masses: a phase I trial. *Lancet Oncol.* 8, 304–310.
- (9) Wadas, T. J., Wong, E. H., Weisman, G. R., and Anderson, C. J. (2007) Copper chelation chemistry and its role in copper radiopharmaceuticals. *Curr. Pharm. Des.* 13, 3–16.
- (10) Zeglis, B., and Lewis, J. S. (2011) A practical guide to the construction of radiometallation bioconjugates for positron emission tomography. *Dalton Trans.*
- (11) Kolb, H. C., Finn, M. G., and Sharpless, K. B. (2001) Click chemistry: diverse chemical function from a few good reactions. *Angew. Chem., Int. Ed.* 40, 2004–2021.
- (12) Lim, R. K. V., and Lin, Q. (2010) Bioorthogonal chemistry: recent progress and future directions. *Chem. Commun.* 46, 1589–1600.
- (13) Sletten, E. M., and Bertozzi, C. R. (2009) Bioorthogonal chemistry: fishing for selectivity in a sea of functionality. *Angew. Chem., Int. Ed.* 48, 6973–6998.
- (14) Moses, J. E., and Moorhouse, A. D. (2007) The growing applications of click chemistry. *Chem. Soc. Rev.* 36, 1249–1262.
- (15) Glaser, M., and Robins, E. G. (2009) 'Click labelling' in PET radiochemistry. *J. Labelled Compd. Radiopharm.* 52, 407–414.
- (16) Mindt, T. L., Muller, C., Stuker, F., Salazar, J. F., Hohn, A., Mueggler, T., Rudin, M., and Schibli, R. (2009) A "click chemistry" approach to the efficient synthesis of multiple imaging probes derived from a single precursor. *Bioconjugate Chem.* 20, 1940–1949.
- (17) Nwe, K., and Brechbiel, M. W. (2009) Growing applications of "click chemistry" for bioconjugation in contemporary biomedical research. *Cancer Biother. Radiopharm.* 24, 289–301.
- (18) Wang, C., Wang, N., Zhou, W., Shen, Y. M., and Zhang, L. (2010) Application of "click chemistry" in synthesis of radiopharmaceuticals. *Progress Chem.* 22, 1591–1602.
- (19) Schultz, M. K., Parameswarappa, S. G., and Pigge, F. C. (2010) Synthesis of a DOTA-biotin conjugate for radionuclide chelation via Cu-free click chemistry. *Org. Lett.* 12, 2398–2401.
- (20) Martin, M. E., Parameswarappa, S. G., O'Dorisio, M. S., Pigge, F. C., and Schultz, M. K. (2010) A DOTA-peptide conjugate by copper-free click chemistry. *Bioorg. Med. Chem. Lett.* 20, 4805–4807.
- (21) Lebedev, A. Y., Holland, J. P., and Lewis, J. S. (2009) Clickable bifunctional radiometal chelates for peptide labeling. *Chem. Commun.* 46, 1706–1708.
- (22) Knor, S., Modlinger, A., Poethko, T., Schottelius, M., Wester, H. J., and Kessler, H. (2007) Synthesis of novel 1,4,7,10-tetraazacyclodecane-1,4,7,10-tetraacetic acid (DOTA) derivatives for chemoselective attachment to unprotected polyfunctionalized compounds. *Chem.—Eur. J.* 13, 6082–6090.
- (23) Devaraj, N. K., Upadhyay, R., Hatin, J. B., Hilderbrand, S. A., and Weissleder, R. (2009) Fast and sensitive pretargeted labeling of cancer cells through a tetrazine/trans-cyclooctene cycloaddition. *Angew. Chem., Int. Ed.* 48, 7013–7016.
- (24) Devaraj, N. K., Weissleder, R., and Hilderbrand, S. A. (2008) Tetrazine-based cycloadditions: application to pretargeted live cell imaging. *Bioconjugate Chem.* 19, 2297–2299.
- (25) Blackman, M. L., Royzen, M., and Fox, J. M. (2008) Tetrazine ligation: fast bioconjugation based on inverse electron demand Diels-Alder reactivity. *J. Am. Chem. Soc.* 130, 13518–13519.
- (26) Schoch, J., Wiessler, M., and Jäschke, A. (2010) Post-synthetic modification of DNA by inverse-electron-demand Diels–Alder reaction. *J. Am. Chem. Soc.* 132, 8846–8847.
- (27) Devaraj, N. K., Hilderbrand, S., Upadhyay, R., Mazitschek, R., and Weissleder, R. (2010) Bioorthogonal turn-on probes for imaging small molecules inside living cells. *Angew. Chem., Int. Ed.* 49.
- (28) Haun, J. B., Devaraj, N. K., Hilderbrand, S., Lee, H., and Weissleder, R. (2010) Bioorthogonal chemistry amplifies nanoparticle binding and enhances the sensitivity of cell detection. *Nat. Nanotechnol.* 5, 660–665.
- (29) Rossin, R., Verkerk, P. R., van den Bosch, S. M., Vuldres, R. C. M., Verel, I., Lub, J., and Robillard, M. S. (2010) In vivo chemistry for pretargeted tumor imaging in live mice. *Angew. Chem., Int. Ed.* 49, 3375–3378.
- (30) Li, Z., Cai, H., Hassink, M., Blackman, M., Brown, R. C. D., Conti, P. S., and Fox, J. M. (2010) Tetrazine-trans-cyclooctene ligation for the rapid construction of 18-F labeled probes. *Chem. Commun.* 46, 8043–8045.
- (31) Reiner, T., Keliher, E. J., Earley, S., Marinelli, B., and Weissleder, R. (2011) Synthesis and in vivo imaging of a 18F-labeled PARP1 inhibitor using a chemically orthogonal scavenger-assisted high-performance method. *Angew. Chem., Int. Ed.* 50, 1922–1925.
- (32) Meijs, W. E., Haisma, H. J., Klok, R. P., vanGog, F. B., Kievit, E., Pinedo, H. M., and Herscheid, J. D. M. (1997) Zirconium-labeled monoclonal antibodies and their distribution in tumor-bearing nude mice. *J. Nucl. Med.* 38, 112–118.
- (33) Meijs, W. E., Herscheid, J. D. M., Haisma, H. J., and Pinedo, H. M. (1992) Evaluation of desferal as a bifunctional chelating agent for labeling antibodies with Zr-89. *Appl. Radiat. Isotop.* 43, 1443–1447.
- (34) Holland, J. P., Divilov, V., Bander, N. H., Smith-Jones, P. M., Larson, S. M., and Lewis, J. S. (2010) Zr-89-DFO-J591 for immunoPET of prostate-specific membrane antigen expression in vivo. *J. Nucl. Med.* 51, 1293–1300.

- (35) Hanahan, D., and Weinberg, R. A. (2000) The hallmarks of cancer. *Cell* 100, 57–70.
- (36) Baselga, J., and Swain, S. M. (2009) Novel anticancer targets: revisiting ERBB2 and discovering ERBB3. *Nat. Rev. Cancer* 9, 463–475.
- (37) Ellis, C. M., Dyson, M. J., Stephenson, T. J., and Maltby, E. L. (2005) HER2 amplification status in breast cancer: a comparison between immunohistochemical staining and fluorescence in situ hybridisation using manual and automated quantitative image analysis scoring techniques. *J. Clin. Pathol.* 58, 710–714.
- (38) Hanahan, D., Weinberg, R. A. Hallmarks of cancer: the next generation. *Cell* 144, 646–674.
- (39) Slamon, D. J., Leyland-Jones, B., Shak, S., Fuchs, H., Paton, V., Bajamonde, A., Fleming, T., Eiermann, W., Wolter, J., Pegram, M., Baselga, J., and Norton, L. (2001) Use of chemotherapy plus a monoclonal antibody against HER2 for metastatic breast cancer that overexpresses HER2. *N. Engl. J. Med.* 344, 783–92.
- (40) Tolmachev, V., Velikyan, I., Sandstrom, M., and Orlova, A. (2010) A HER2-binding Affibody molecule labelled with Ga-68 for PET imaging: direct in vivo comparison with the In-111-labelled analogue. *Eur. J. Nucl. Med. Mol. Imaging* 37, 1356–1367.
- (41) Tang, Y., Wang, J., Scollard, D. A., Mondal, H., Holloway, C., Kahn, H. J., and Reilly, R. M. (2005) Imaging of HER2/neu-positive BT-474 human breast cancer xenografts in athymic mice using 111In-trastuzumab (Herceptin) Fab fragments. *Nucl. Med. Biol.* 32, 51–58.
- (42) Holland, J. P., Caldas-Lopes, E., Divilov, V., Longo, V. A., Taldone, T., Zatorska, D., Chiosis, G., and Lewis, J. S. (2010) Measuring the pharmacodynamic effects of a novel Hsp90 inhibitor on HER2/neu expression in mice using Zr-89-DFO-trastuzumab. *PLOS One* 5.
- (43) Munnink, T. H. O., de Korte, M. A., Nagengast, W. B., Timmer-Bosscha, H., Schroder, C. P., de Jong, J. R., van Dongen, G., Jensen, M. R., Quad, C., Lub-de Hooge, M. N., and de Vries, E. G. E. (2010) Zr-89-trastuzumab PET visualises HER2 downregulation by the HSP90 inhibitor NVP-AUY922 in a human tumour xenograft. *Eur. J. Cancer* 46, 678–684.
- (44) Dijkers, E. C. F., Kosterink, J. G. W., Rademaker, A. P., Perk, L. R., van Dongen, G. A. M. S., Bart, J., de Jong, J. R., de Vries, E. G. E., and Lub-de Hooge, M. N. (2009) Development and characterization of clinical-grade <sup>89</sup>Zr-trastuzumab for HER2/neu immunolPET imaging. *J. Nucl. Med.* 50, 974–981.
- (45) Niu, G., Li, Z., Cao, Q., and Chen, X. (2009) Monitoring therapeutic response of human ovarian cancer with 17-DMAG by noninvasive PET imaging with <sup>64</sup>Cu-DOTA-trastuzumab. *Eur. J. Nucl. Med. Mol. Imaging*.
- (46) Smith-Jones, P. M., Solit, D. B., Afroze, F., Rosen, N., and Larson, S. M. (2006) Early tumor response to Hsp90 therapy using HER2 PET: Comparison with 18F-FDG PET. *J. Nucl. Med.* 47, 793–796.
- (47) Garmestani, K., Milenic, D. E., Plascjak, P. S., and Brechbiel, M. W. (2002) A new and convenient method for purification of <sup>86</sup>Y using a Sr(II) selective resin and comparison of biodistribution of <sup>86</sup>Y and <sup>111</sup>In labeled Herceptin. *Nucl. Med. Biol.* 29, 599–606.
- (48) Verel, I., Visser, G. W. M., Boellaard, R., Stigter-van Walsum, M., Snow, G. B., and van Dongen, G. (2003) Zr-89 immuno-PET: Comprehensive procedures for the production of Zr-89-labeled monoclonal antibodies. *J. Nucl. Med.* 44, 1271–1281.
- (49) Zanzonico, P. (2009) Routine quality control of clinical nuclear medicine instrumentation: a brief review. *J. Nucl. Med.* 49, 1114–1131.
- (50) McCarthy, D. W., Shefer, R. E., Klinkowstein, R. E., Bass, L. A., Margeneau, W. H., Cutler, C. S., Anderson, C. J., and Welch, M. J. (1997) Efficient production of high specific activity Cu-64 using a biomedical cyclotron. *Nucl. Med. Biol.* 24, 35–43.
- (51) Holland, J. P., Sheh, Y. C., and Lewis, J. S. (2009) Standardized methods for the production of high specific-activity zirconium-89. *Nucl. Med. Biol.* 36, 729–739.
- (52) Anderson, C. J., Connett, J. M., Schwarz, S. W., Rocque, P. A., Guo, L. W., Philpott, G. W., Zinn, K. R., Meares, C. F., and Welch, M. J. (1992) Copper-64-labeled antibodies for PET imaging. *J. Nucl. Med.* 33, 1685–1691.
- (53) Anderson, C. J., Schwarz, S. W., Connett, J. M., Cutler, P. D., Guo, L. W., Germain, C. J., Philpott, G. W., Zinn, K. R., Greiner, D. P., Meares, C. F., and Welch, M. J. (1995) Preparation, biodistribution, and dosimetry of copper-64-labeled anti-colorectal carcinoma monoclonal antibody fragments 1A3-F(AB')(2). *J. Nucl. Med.* 36, 850–858.
- (54) Lindmo, T., Boven, E., Cuttitta, F., Fedorko, J., and Bunn, P. A., Jr. (1984) Determination of the immunoreactive fraction of radiolabeled monoclonal antibodies by linear extrapolation to binding at infinite antigen excess. *J. Immunol. Methods* 72, 77–89.
- (55) Lindmo, T., and Bunn, P. A., Jr. (1986) Determination of the true immunoreactive fraction of monoclonal antibodies after radiolabeling. *Methods Enzymol.* 121, 678–91.
- (56) Kim, J. S., Lee, J. S., Im, K. C., Kim, S. J., Kim, S.-Y., Lee, D. S., and Moon, D. H. (2007) Performance measurement of the microPET Focus 120 scanner. *J. Nucl. Med.* 48, 1527–1535.
- (57) Kampchen, T., Massa, W., Overheu, W., Schmidt, R., and Seitz, G. (1982) Zur kenntnis von reaktionen des 1,2,4,5-tetrazin-3,6-dicarbon-saure-dimethylesteren mit nucleophilen. *Chem. Ber.* 115, 683–694.
- (58) Lin, C. H., Lieber, E., and Horwitz, J. P. (1954) The synthesis of syn-diaminotetrazine. *J. Am. Chem. Soc.* 76, 427–430.
- (59) Solducho, J., Doskocz, J., Cabaj, J., and Roszak, S. (2003) Practical synthesis of bis-substituted tetrazine with two pendant 2-pyrrolyl or 2-thienyl groups, precursors of new conjugated polymers. *Tetrahedron* 59, 4761–4766.
- (60) Vosjan, M., Perk, L. R., Visser, G. W. M., Budde, M., Jurek, P., Kiefer, G. E., and van Dongen, G. (2010) Conjugation and radiolabeling of monoclonal antibodies with zirconium-89 for PET imaging using the bifunctional chelate p-isothiocyanatobenzyl-desferrioxamine. *Nat. Protoc.* 5, 739–743.
- (61) Verel, I., Visser, G. W. M., Boellaard, R., Stigter-van Walsum, M., Snow, G. B., and van Dongen, G. A. M. S. (2003) <sup>89</sup>Zr immuno-PET: comprehensive procedures for the production of <sup>89</sup>Zr-labeled monoclonal antibodies. *J. Nucl. Med.* 44, 1271–1281.
- (62) Brouwers, A., Verel, I., Van Eerd, J., Visser, G., Steffens, M., Oosterwijk, E., Corstens, F., Oyen, W., Van Dongen, G., and Boerman, O. (2004) PET radioimmunoscinigraphy of renal cell cancer using Zr-89-labeled cG250 monoclonal antibody in nude rats. *Cancer Biother. Radiopharm.* 19, 155–163.
- (63) Niu, G., Li, Z., Xie, J., Le, Q.-T., and Chen, X. (2009) PET of EGFR antibody distribution in head and neck squamous cell carcinoma models. *J. Nucl. Med.* 50, 1116–1123.
- (64) Martin, S. M., O'Donnell, R. T., Kukis, D. L., Abbey, C. K., McKnight, H., Sutcliffe, J. L., and Tuscano, J. M. (2008) Imaging and pharmacokinetics of <sup>64</sup>Cu-DOTA-HB22.7 administered by intravenous, intraperitoneal, or subcutaneous injection to mice bearing non-Hodgkin's lymphoma xenografts. *Mol. Imaging Biol.* 11, 79–87.
- (65) Paudyal, P., Paudyal, B., Hanaoka, H., Oriuchi, N., Iida, Y., Yoshioka, H., Tominaga, H., Watanabe, S., Ishioka, N. S., and Endo, K. (2010) Imaging and biodistribution of Her2/neu expression in non-small cell lung cancer xenografts with <sup>64</sup>Cu-labeled trastuzumab PET. *Cancer Sci.* 101, 1045–1050.
- (66) Abou, D. S., Ku, T., and Smith-Jones, P. M. (2011) In vivo biodistribution and accumulation of <sup>89</sup>Zr in mice. *Nucl. Med. Biol.* [Online early access].
- (67) Antunes, P., Ginj, P., Zhang, H., Waser, B., Baum, R. P., Reubi, J. C., and Maecke, H. (2007) Are radiogallium-labeled DOTA-conjugated somatostatin analogues superior to those labeled with other radiometals? *Eur. J. Nucl. Med. Mol. Imaging* 34, 982–993.